AD-A122 138 DESIGN CONSIDERATIONS IN THE EMPLOYMENT OF RARE EARTH-COBALT PERMANENT MA..(U) ARMY ELECTRONICS RESEARCH AND DEVELOPMENT COMMAND FORT MONMOU.. 1/1

UNCLASSIFIED H A LEUPOLD NOV 82 DELET-TR-82-9 F/G 20/3 NL

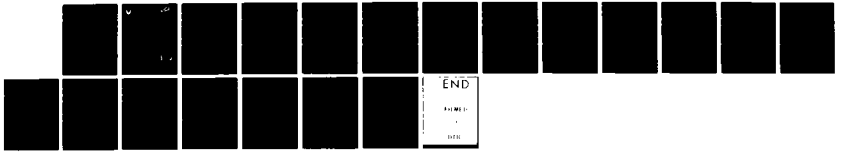

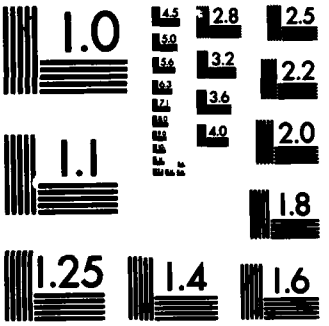

RESEARCH AND DEVELOPMENT TECHNICAL REPORT

DELET-TR-82-9

DESIGN CONSIDERATIONS IN THE EMPLOYMENT OF RARE EARTH-COBALT PERMANENT MAGNETS AS FLUX SOURCES

HERBERT A. LEUPOLD
ELECTRONICS TECHNOLOGY & DEVICES LABORATORY

NOVEMBER 1982

ERADCOM

US ARMY ELECTRONICS RESEARCH & DEVELOPMENT COMMAND
FORT MONMOUTH, NEW JERSEY 07703

NOTICES

Disclaimers

The citation of trade names and names of manufacturers in this report is not to be construed as official Government indorsement or approval of commercial products or services referenced herein.

Disposition

Destroy this report when it is no longer needed. Do not return it to the originator.

UNCLASSIFIED

SECURITY CLASSIFICATION OF THIS PAGE (When Data Entered)

REPORT DOCUMENTATION PAGE		READ INSTRUCTIONS BEFORE COMPLETING FORM
1. REPORT NUMBER DELET-TR-82-9	2. GOVT ACCESSION NO. AD-A122 138	3. RECIPIENT'S CATALOG NUMBER
4. TITLE (and Subtitle) DESIGN CONSIDERATIONS IN THE EMPLOYMENT OF RARE EARTH-COBALT PERMANENT MAGNETS AS FLUX SOURCES		5. TYPE OF REPORT & PERIOD COVERED 6. PERFORMING ORG. REPORT NUMBER
7. AUTHOR(s) Herbert A. Leupold		8. CONTRACT OR GRANT NUMBER(s)
9. PERFORMING ORGANIZATION NAME AND ADDRESS US Army Electronics Technology and Devices Laboratory (ERADCOM) Fort Monmouth, NJ 07703		10. PROGRAM ELEMENT, PROJECT, TASK AREA & WORK UNIT NUMBERS 611101A 1L161101A91A 4909
11. CONTROLLING OFFICE NAME AND ADDRESS Electronic Materials Research Division US Army Electronics Technology and Devices Lab (ERADCOM) Fort Monmouth, NJ 07703 DELET-ES		12. REPORT DATE November 1982 13. NUMBER OF PAGES 15
14. MONITORING AGENCY NAME & ADDRESS(if different from Controlling Office)		15. SECURITY CLASS. (of this report) UNCLASSIFIED 15a. DECLASSIFICATION/DOWNGRADING SCHEDULE

16. DISTRIBUTION STATEMENT (of this Report)

Approved for public release; distribution unlimited.

17. DISTRIBUTION STATEMENT (of the abstract entered in Block 20, if different from Report)

18. SUPPLEMENTARY NOTES

19. KEY WORDS (Continue on reverse side if necessary and identify by block number)

high coercivity; linear demagnetization curves; magnetic analogue of Ohm's law; energy product; equivalent pole distributions

20. ABSTRACT (Continue on reverse side if necessary and identify by block number)

The design advantages resulting from the linear demagnetization curves of rare-earth permanent magnets are discussed. The magnetic analogue to Ohm's law is derived and its affiliation illustrated by an example. Other aspects of design, such as the replacement of magnetic circuits with equivalent pole densities and the significance of the energy product, are also discussed.

DD FORM 1 JAN 73 1473 EDITION OF 1 NOV 65 IS OBSOLETE

UNCLASSIFIED

SECURITY CLASSIFICATION OF THIS PAGE (When Data Entered)

CONTENTS

TABLE

FIGURES

Design Considerations in the Employment of Rare-Earth Cobalt Permanent Magnets as Flux Sources

INTRODUCTION

The advent of rare earth-cobalt permanent magnets (REPM's) affords the possibility of fabrication of many novel magnetic structures that are not otherwise practicable. So different are these remarkable materials from conventional magnets that the conventional design wisdom is inadequate to fully exploit their unique characteristics. Indeed, the conventional wisdom can lead to error or to the employment of cumbersome procedures appropriate for conventional magnets but unnecessary for REPM's. All of these salutary characteristics stem from two basic attributes of the rare earth-cobalt materials:

(1) large intrinsic moments per unit volume (high saturation magnetizations);

(2) extraordinarily high resistance to demagnetization by applied fields or demagnetization fields (high coercivity).

The first provides a magnetic field source of high flux density; the second enables the magnet to maintain this flux density in the face of very high demagnetizing fields engendered by low-aspect ratios. Thus, REPM's can, with impunity, be fashioned into shapes that would cause demagnetization of conventional materials.

This point is illustrated in Figure 1 which shows the second quadrant of the hysteresis loop of a typical $SmCo_5$ magnet. Note that the constancy of magnetization to the very high field of 10 kOe results in a linear B vs. H curve of slope one throughout the entire quadrant. Further, since no self-demagnetizing field arising from magnet geometry can ever exceed B_r = 9000 oersteds, and since more than 10,000 oersteds are needed to reduce the magnetization, no $SmCo_5$ magnet can be affected by self-demagnetization.

The importance of this property to design simplification will become obvious from the following discussions.

THE MAGNETIC ANALOGUE TO OHM's LAW

In the not-too-distant past, elementary courses in general physics almost invariably included a brief treatment of magnetic circuits which featured a rather simplistically derived magnetic analogue of Ohm's law. In this scheme, the roles of electric current I, electromotive force V, electric conductance G, and resistance R were played, respectively, by the magnetic flux ϕ, the magneto-motive force F, the magnetic permeance P, and the reluctance R, so that the magnetic Ohms' law read

$$\phi = PF \quad \text{or} \quad \phi = F/R \,, \tag{1}$$

just as in the case of the corresponding electric circuit equations. Permanent magnets then acted as magnetic "batteries," materials of high permeability, such as soft iron or permalloy as essentially perfect flux conductors, and air gaps or materials of low permeability as magnetic "resistors." The analogy was completed by the option of winding electric coils around permeable members of a circuit, thus producing flux generators, either dc or ac, according to the current sent through the coils.

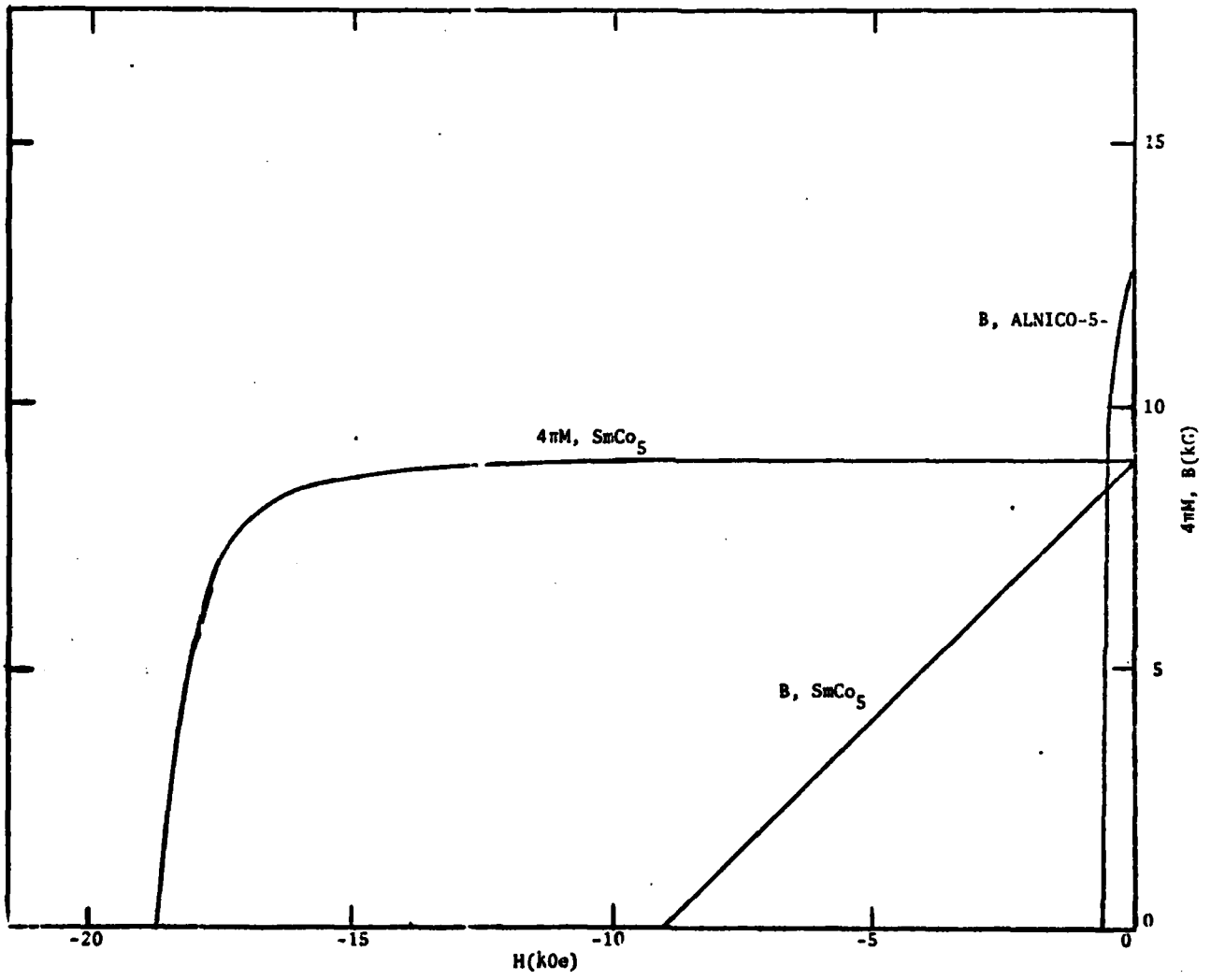

Figure 1. Demagnetization curves for $SmCO_5$ and ALNICO-5 magnets.

Although this approach, as in most analogies, was philosophically and mnemonically gratifying, it was rarely used in practice, as outlined; mention of it is now often deleted from the elementary courses. The barrier to more general usefulness was essentially twofold. First, unlike electric currents, magnetic fluxes are not confined to neat, analytically tractable paths like wires, but fill virtually all of space. This difficulty was less serious because the space around a magnetic circuit can, in many cases, be divided into flux paths of which the boundaries are planes, cylindrical arcs, or spherical segments that emanate normally from the surfaces of the circuit to connect points of different magnetic potential. The permeances of these simplified paths can then be calculated through standard formulae and, if the division has been judiciously made, surprisingly good approximations to the true fluxes can often be obtained.

The second, and more serious, difficulty that in the past has prevented a simple direct application of the magnetic Ohm's law is that conventional permanent magnet materials, such as the Alnico's, generate no unique magnetomotive (MMF) force because their MMF's depend upon the circuits into which they are inserted. The great value of REPM's in the simplification of the circuit design process arises because these materials exhibit the same total circuital MMF regardless of the natures of the circuits in which they find themselves. Although this advantage has been discussed previously,[1,2] it is still not as widely appreciated as are the high energy products and coercivities of the rare earth-cobalts, and, consequently, circuits employing these materials are still often analyzed by the same cumbersome procedures necessary when conventional materials are employed.

To illuminate the origins of these difficulties and to highlight the contrasts between the cobalt rare earths and conventional magnets, it is useful to consider the derivation of the magnetic Ohm's law. We begin by writing the circuital form of Ampere's law:

$$\oint \vec{H} \cdot d\vec{\ell} = \pm \frac{4\pi n I}{10} \tag{2}$$

where H is in oersteds, I is in amperes, and the sign depends upon whether the current direction in the coils produces an MMF aiding or opposing that of the magnet. Assuming H_m is the average field over the length of the magnet ℓ_m, we can write

$$H_m \ell_m + \int_A^B \vec{H}_L \cdot d\vec{\ell} = \frac{4\pi n I}{10} \quad , \tag{3}$$

where A and B are the ends of the magnet, the line integral is along a flux line outside of the magnet and H_L is the field along that line integral.

1. A. E. Paladino, N. J. Dionne, P. F. Weihrauch, and E. C. Wettstein, "Rare Earth-Cobalt Permanent Magnet Technology," Goldschmidt Informient Nr 35, p. 63 (1975).

2. H. A. Leupold and F. Rothwarf, "Design of a Tuneable Magnetic Circuit for K and Ka Band Microwave Filters," Proceedings of the Second International Workshop on Rare Earth-Cobalt Permanent Magnets and Their Applications, pp. 187 (1976).

Outside the magnet $\mu_L H_L + B_L$, therefore,

$$H_m \ell_m + \int_A^B \vec{B}_L \frac{\cdot d\vec{\ell}}{\mu_L} = \pm \frac{4\pi nI}{10} \quad , \tag{4}$$

but

$$B_L = \frac{d\Phi(r)}{dA} \tag{5}$$

where dA is a differential element of area normal to a flux line of length ℓ and $d\Phi(r)$ is the flux passing through it. Consequently,

$$H_m \ell_m + \int_A^B \frac{d\Phi(r)}{dA} \frac{d\ell}{\mu_L} = \pm \frac{4\pi nI}{10} \tag{6}$$

$$H_m \ell_m + \left(\overline{\frac{d\Phi}{\mu_L dA}}\right)\ell = \pm \frac{4\pi nI}{10} \quad . \tag{7}$$

The area dA and permeability μ_L associated with flux $d\Phi$ will, of course, vary as we go along the flux line, but if we denote the average product by $\mu_L dA$ and write

$$\left(\overline{\frac{d\Phi}{\mu_L dA}}\right) = \frac{d\Phi}{\mu_L dA} \quad ,$$

then

$$\frac{\ell}{\mu_L dA} = \frac{1}{dP_t^E} \tag{8}$$

where P_t^E is the total permeance of the circuit exclusive of the internal permeance of the magnet.

Equation (7) becomes

$$H_m \ell_m + \frac{d\Phi}{dP_t^E} = \pm \frac{4\pi nI}{10} \tag{9}$$

$$\frac{d\Phi}{dP_t^E} = \pm \frac{4\pi nI}{10} - H_m \ell_m \quad . \tag{10}$$

Integrating all fluxes, $d\phi$, yields

$$\frac{\phi_t}{\substack{E \\ P_t}} = \pm\frac{4\pi nI}{10} - H_m\ell_m \tag{11}$$

where ϕ_t is the total flux emanating from the magnet, ϕ_m; therefore,

$$\phi_m = \phi_t = P_t^E \left[\pm\frac{4\pi nI}{10} - H_m\ell_m\right]. \tag{12}$$

However,

$$\phi_m = B_m A_m \quad , \tag{13}$$

where B_m is the average flux density within the magnet, and by substituting (13) in (12) we obtain

$$B_m = \frac{P_t^E}{A_m}\left[\pm\frac{4\pi nI}{10} - H_m\ell_m\right] \quad . \tag{14}$$

For $SmCo_5$ the demagnetization curve is reversible, linear, and of the form

$$B_m = \mu_R H_m + B_r \tag{15}$$

where μ_R is the recoil permeability.

Solving (13) and (15) for H_m, we get

$$H_m = \frac{B_m - B_r}{\mu_R} = \frac{\phi_m}{\mu_R A_m} - \frac{B_r}{\mu_R} \quad . \tag{16}$$

Multiplying (14) through by A_m and combining the results with (16) yields

$$\phi_m = P_t^E\left[\frac{-\phi_m\ell_m}{\mu_R A_m} + \frac{B_r}{\mu_R}\ell_m \pm \frac{4\pi nI}{10}\right] \tag{17}$$

$$\phi_m = \frac{\frac{B_r}{\mu_R}\ell_m \pm \frac{4\pi nI}{10}}{\frac{1}{P_t^E} + \frac{\ell_m}{\mu_R A_m}} \tag{18}$$

and

$$\phi_m = \frac{\frac{B_r}{\mu_R}\ell_m \pm \frac{4\pi nI}{10}}{R_t^E + R_m} \quad . \tag{19}$$

This is the magnetic form of Ohm's law where the total flux is analogous to the total current and the reluctances R_t^E amd R_m correspond to the total external circuit resistance and battery internal resistance, respectively. $\frac{B_r}{\mu R_a}\ell_m$ corresponds to the battery EMF and $\pm \frac{4\pi nI}{10}$ is the analogue of the EMF from zero impedance, constant voltage source.[10] This simple and useful formula is applicable to cobalt rare earth magnets because of the linear relationship between H_m and B_m expressed by equation (15) which, in turn, is a consequence of the constancy of magnetization in all parts of the magnet regardless of stimuli arising from the rest of the circuit or the magnet's own geometrical peculiarities. In contrast, conventional magnetic materials do not have reversible demagnetization curves that are expressible in simple analytical form. Therefore, in dealing with circuits containing such magnets one must proceed less directly and with recourse to B-H graphs such as shown in Figure 2. For simplicity, we consider as an example a circuit with no electromagnetic sources of flux. In such a case, equation (14) can be written:

$$\frac{B_m}{H_m} = \frac{\ell_m}{A_m} p_t^E \quad . \tag{20}$$

Then one must calculate P_t^E which, together with the use of magnet length and cross section area in (20), yields B_m/H_m. Then a "load line" with slope B_m/H_m is drawn through the origin and its intersection with the second quadrant B-H curve determines B_m. The product $B_m A_m$ then yields Φ_t which is the total flux output of the magnet; Φ_t can then be distributed among the various flux paths in the circuit in accordance with Ohm's and Kirchoff's laws.

If the demagnetization field of the conventional magnet is lessened by an increase in P_t^E resulting from the narrowing of an air gap within the circuit, the operating point of the magnet moves along an approximately linear minor loop to point B in Figure 2, in accordance with the new value of B_m/H_m. Since changes in the circuit are such as to move the operating point from left to right on the minor loop, we can use an expression such as (15) with the intercept of the minor loop with the B axis, B_i in place of B_r, and the slope of the minor loop μ_r in place of μ_R. One may then define a magnet MMF of the same form as that for the cobalt- rare earths, i.e.,

$$F = B_i \ \ell_m/\mu_r \quad . \tag{21}$$

However, should the demagnetization field increase due to a widening of an airgap, temporary removal of the magnet from the circuit or application of an external demagnetizing field, the operating point would move to the left along the demagnetization curve to C, the base of a new minor loop CD. The magnet would then also have a new MMF given by the new line constants B_i' and μ_r'

$$F' = B_i' \ \ell_m/\mu_r' \quad . \tag{22}$$

Hence, we see that no unique MMF can be assigned to a conventional permanent magnet, and if the useful magnetic field is to be modulated by variation of gap length or electrically generated MMF's, the magnet MMF will always be that corresponding to the lowest point on the demagnetization curve reached in the course of the modulation cycles. An additional complication in determining the MMF of a conventional magnet is that the lengths, ℓ_m, appearing in equations (21) and (22) are effective rather than actual lengths. Because of demagnetization fields, the magnetization of conventional magnets tends to be nonuniform, which means that different parts of the magnet lie on different load lines, hence producing different MMF's and inhomogeneous fields. This causes effective lengths to be shorter than

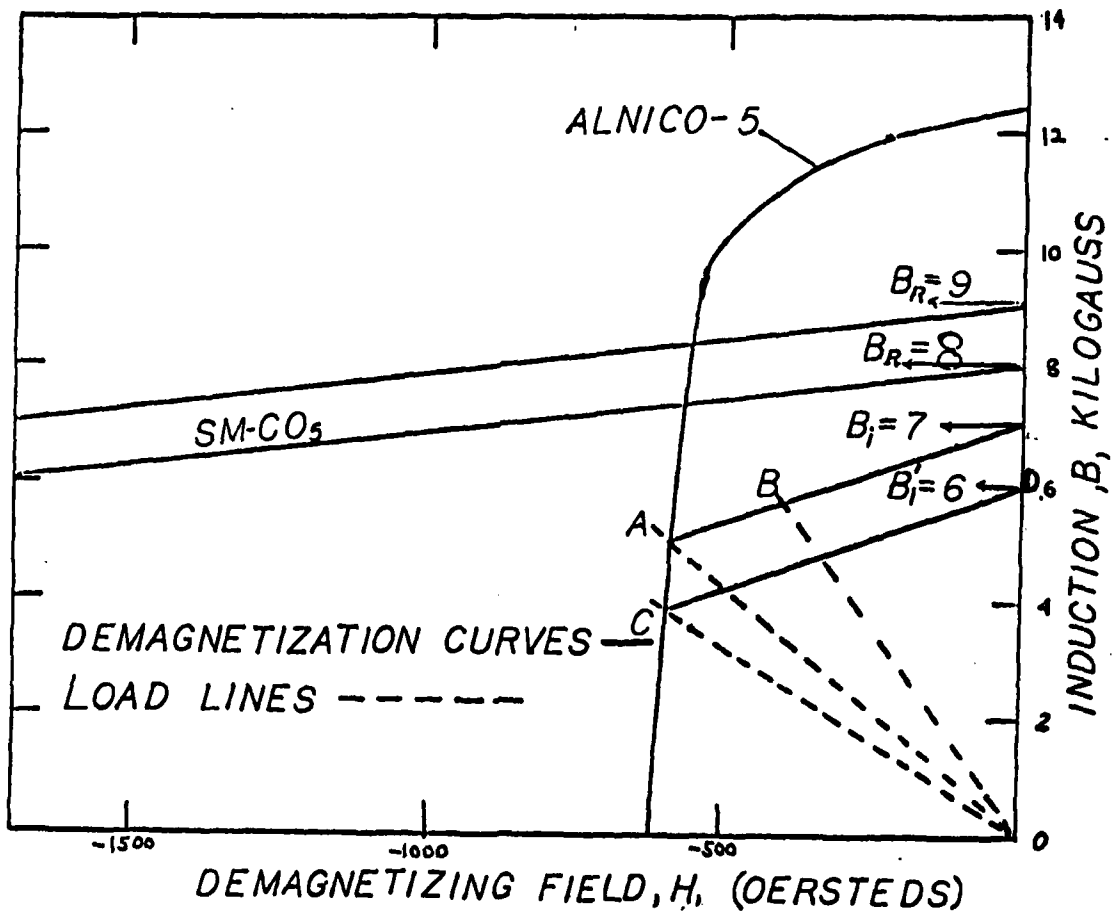

Figure 2. Determination of B_m in an Alnico 5 Magnet. The load line, OA, is determined from the total external permeance as described in the text. B_m is the value of B at intersection A. If P_t would lower the operating point to C, the base of a new reversible minor loop CD. The reversible linear demagnetization curves for $SmCo_5$ magnets of B_r = 8 and 9 kG are shown for purposes of comparison.

actual ones and all the other germane quantities such as H_m, B_m to have only a rough average significance. For some configurations, use of geometrical lengths and average field values can cause significant errors, and estimations of effective lengths must be made. For an example, see Reference 3.

SIGNIFICANCE OF THE ENERGY PRODUCT

If one combines the leakage paths of a magnetic circuit with a gap in which the flux is to be maximized, the circuit can be represented by the schematic of Figure 3. The magnetic circuit analogue to electric power is magnetic field energy, and the amount stored in the gap is given by

$$E_g = F_g \phi = H_g L_g A_g B_g = H_g B_g V_g \tag{23}$$

Again, in analogy with electric circuit theory, we know that this quantity will be maximized when the proper impedances are matched, that is, when

$$R_g = \frac{R_L R_m}{R_L + R_m} \tag{24}$$

where R_L is the external load reluctance exclusive of R_g. The slope of the load line is given by

$$S = B_m/H_m = P_t^E \frac{\ell_m}{A_m} = P_t^E R_m \quad , \tag{25}$$

$$S = [P_g + P_L] \quad . \tag{26}$$

Substituting (24) in (26) we obtain

$$S = [1 + R_m/R_L + \frac{1}{R_L}] \quad .$$

Under the ideal condition of no leakage,

$$R_L = \infty \text{ and } S = 1.$$

However, at $S = 1$, $B_m = H_m = B_r/2 = H_c/2$ and

$$H_g = B_g = \frac{B_m \ell_g}{A_g(R_g + R_m)} = \frac{H_c \ell_g}{2A_g (R_g + R_m)} \quad . \tag{27}$$

Thus, (23) becomes

$$E_g = \frac{B_m H_c \ell_g^2 V_g}{2A_g^2 (R_g + R_m)^2} = \frac{B_r H_c \ell_g^2 V_g}{4A_g^2 (R_g + R_m)^2} \tag{28}$$

3. R. J. Parker and R. J. Studders, Permanent Magnets and Their Application (John Wiley and Sons, Inc., New York - London 1962), pp. 130-150.

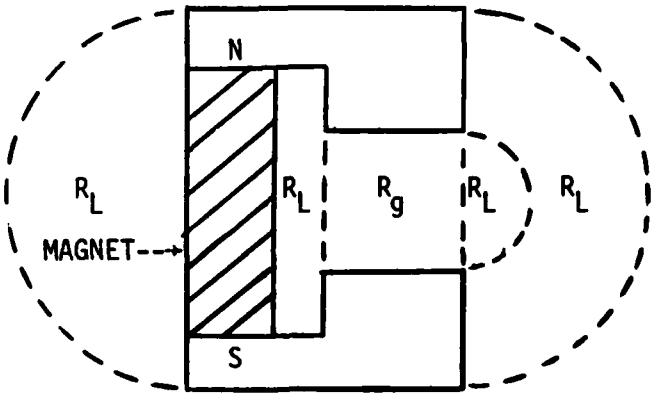

A.

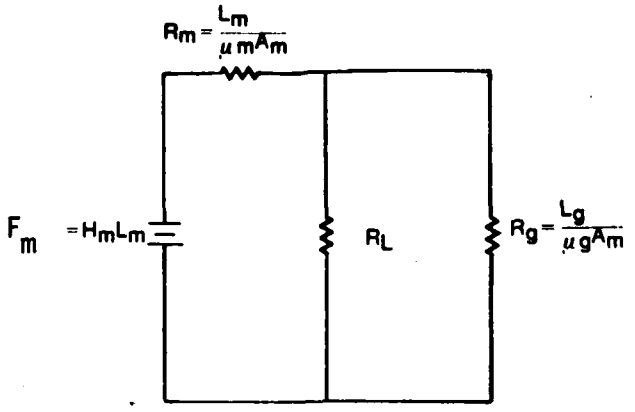

B.

Figure 3. Permanent magnet circuit (A) and schematic of equivalent electrical circuit (B).

and

$$E_g = \frac{B_r H_c V_g}{4} \frac{1}{[1 + R_m/R_g]} 2 \quad . \tag{29}$$

The factor $B_r H_c/4$ is called the "energy product" of the material under consideration and, as shown by (29), is a measure of the maximum field energy that the material can store in a gap under ideal conditions. As Figure 1 shows, it is just equal to one half the area under the B-H loop in the second quadrant. The graph also shows that the area for Alnico 5 is much smaller, which is indicative of the ability of $SmCo_5$ to produce much larger fields in larger working volumes.

EQUIVALENT SURFACE AND VOLUME POLE DISTRIBUTIONS

Because a uniformly magnetized REPM retains that state under placement into any magnetic circuit, for computational purposes it can always be replaced by the pole density distribution on its surfaces which is given by

$$\sigma = \hat{n} . \vec{M} \quad , \tag{30}$$

where $\vec{M}$ is the magnetization everywhere in the body of the magnet and $\hat{n}$ is the unit vector normal to the surface of the magnet. For simple configurations such as those with geometric and magnetic cylindrical symmetry, it is often useful to replace nonuniform magnetizations with equivalent volume pole distributions where the pole density is given by

$$\rho = -\nabla \cdot \vec{M} \quad . \tag{31}$$

Figure 4 shows some permanent magnet configurations together with their equivalent pole distributions. All can be solved exactly for points lying on the axis of symmetry by integration of Coulomb's expression for field over the pole distributions. Replacement of REPM's by equivalent pole distributions is often useful for quick qualitative checks on the relative efficacy of alternative configurations. For example, it is clear from Figure 4 that the greater number of poles in proximity to point O' in configuration B will produce a larger field there than will be produced by the pole distribution of configuration A at the equivalent point O. Such easy comparisons are not possible when conventional magnets are used because of the complications introduced by volume charge densities that invariably arise because of nonuniform magnetizations due to demagnetization effects. The presence of passive magnetic materials such as iron or permalloy will introduce similar complications even when REPM's are used, but these can sometimes be circumvented by standard field computational techniques such as the method of mirror images. For some problems, a preferable alternative might be to view the REPM system as consisting of either an equivalent array of current sheets or a volume distribution of dipoles. Again, neither of these alternatives is easily feasible when conventional magnets are used.

SUMMARY

From the foregoing considerations, it is clear that designing circuits with conventional magnets is like engaging in electrical circuit design with batteries the cells of which produce different EMF's, and of which the total EMF's and internal resistances depend upon the circuits in which they are placed, as well as upon their previous histories. These difficulties can be mostly obviated by the use of cobalt-rare earth magnets that constitute true magnetic "batteries." These can be standardized to produce definite MMF's measured in gilberts and internal reluctances measured in centimeters^{-1}, much as the EMF's and internal resistances of electrical batteries are rated in volts and ohms, respectively. As is further demonstrated by the

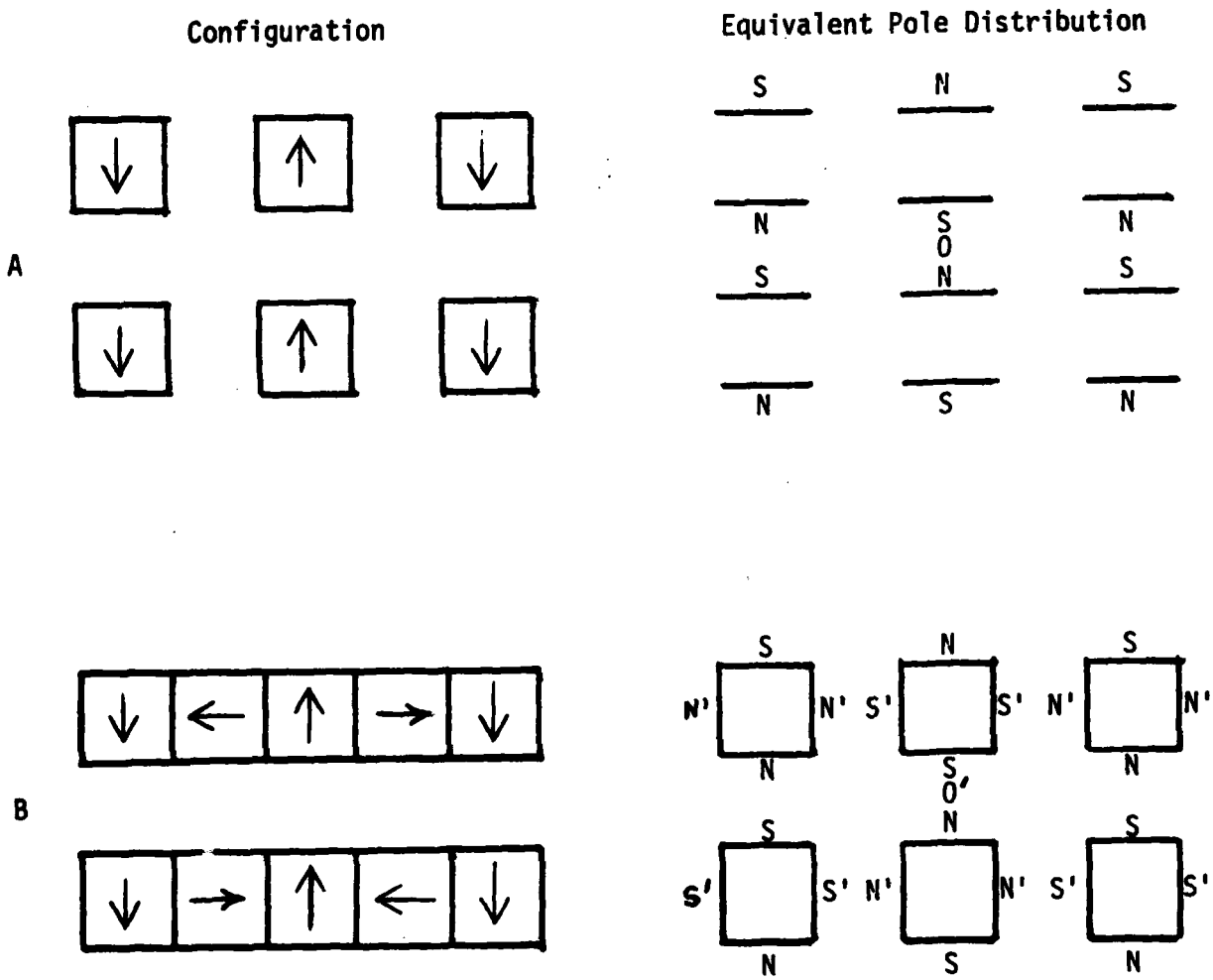

Figure 4. Reduction of magnet arrangements to equivalent pole distribution. The left side of A illustrates the cross section of a segment of a planar periodic stack of $SmCo_5$ permanent magnets that are oriented perpendicularly to the plane of the stack. The right side of A shows the equivalent pole distribution of that configuration. N and S are surface poles of density $\sigma = \vec{M} \cdot \hat{n}$ where $\vec{M}$ is the magnetization vector and $\hat{n}$ the unit vector normal to a magnet surface. The left side of B illustrates the same configuration with the addition of magnets oriented in the plane of the stack, as shown, so as to fill the spaces between the normally oriented magnets. As shown at the right side of B, the resulting pole distribution is that of A with the addition of surface poles N' and S'. Clearly, these would add to the field at point O.

example in the appendix, this property of REPM's greatly simplifies the process of preliminary circuit design in which the estimation of permeance is used, especially in that it eliminates the need for plotting load lines in the second quadrant of a magnet's demagnetization curve. All one needs to solve many circuit problems in this way is a knowledge of the standard permeance formulae[4] and the value of B_r for the REPM to be used. Both experiment and more exact computer calculations used to obtain the fine details of the fields and fluxes of designs roughly arrived at by the Ohms's law method usually show fair ($\sim$ 30%) and often excellent (2%) agreement with the results of the latter method.[5,6] In addition to the high energy products and flux densities produced by REPM's, there are other advantages arising from their use, notably the following simplifications of design:

(1) constancy of MMF, regardless of the configuration of the magnetic circuit in question and the augmentation of the utility of the method of estimation of permeances thus engendered;

(2) persistence of constant uniform magnetization in the face of high demagnetization fields arising from unfavorable aspect ratios;

(3) good approximation of the geometrical length of an REPM to the effective magnetic length used in computing the MMF;

(4) the possibility of simplification of field calculations by the replacement of REPM with equivalent surface pole densities, current sheets or volume dipole distributions.

4. H. C. Roters, Electromagnetic Devices (John Wiley and Sons, Inc., London: Chapman & Hall, Limited) pp. 130-150.

5. H. A. Leupold, F. Rothwarf, C. J. Campagnuolo, H. Lee, and J. E. Fine, "Magnetic Circuit Design Studies for an Inductive Sensor," Tech. Report ECOM-4158, Fort Monmouth, NJ, October 1973.

6. H. A. Leupold, F. Rothwarf, D. Edmiston, C. J. Campagnuolo, H. Lee, J. E. Fine, "A Flux Circuit Analysis for the Magnetic Transducer of a Fluidic Reed Generator," Tech. Report ECOM-4284, p. 27, Fort Monmouth, NJ (1975).

APPENDIX - ILLUSTRATIVE EXAMPLE OF CONTRASTING MAGNETIC GAP FIELD CALCULATIONS FOR A CIRCUIT EMPLOYING $SmCo_5$ AND THE SAME CIRCUIT USING ALNICO 5

In Figure 5a is pictured a simple magnetic circuit with the space around it divided into permeance paths as described in the introduction. The flux and field of interest is that in the magnet gap P_G. To calculate these quantities we must first find the permeance associated with the fourteen flux paths. All are of standard form and can be calculated by means of formulae found in Reference 4. To aid in the visualization of the forms of these paths, brief descriptions of each are summarized in Table 1. All of the fourteen permeances are in parallel with each other and in series with the internal permeance, P_M, of the magnet (see Figure 4B). From the values of the quantitites shown, the total circuit reluctance is given by $R_t = R_M + R_t^E = 0.037 + 0.311 = 0.348\ cm^{-1}$.

The MMF:

$$F = \ell_m B_r / M_R = 3.96\ B_r/1.05 = 3.77\ B_r \text{ gilberts} \quad .$$

From Ohm's law we find the total flux emanating from the magnet:

$$\phi_t = F/R_t = 3.77\ B_r/0.348 = 10.8\ B_r \text{ maxwells.}$$

Since all permeances in P_t^E are in parallel, the gap flux is given by:

$$\phi_G = P_G\ \phi_t/P_t^E = (10.1)(10.8)\ B_r/26.8$$

$$\phi_G = 4.04\ B_r \text{ maxwells.}$$

Hence, if we choose the typical value of Br = 9kG for commercial $SmCo_5$, we have:

$$\phi_G = 9X4.04 = 36.4 \text{ kilomaxwells}$$

and the average gap field

$$\overline{B}_G = \phi_G/A_G = 36.4/19.4 = 1.87 \text{ kilogauss.}$$

If the calculation were to be made for the same configuration with the $SmCo_5$ replaced by Alnico 5, one would proceed as follows:

(1) Calculate the total external permeance $P_t^E = 26.8$ cm and total circuit permeance $P_t = 2.87$ cm.

(2) Find the ratio $\overline{B}_m/\overline{H}_m$ via the formula

$$\overline{B}_m/\overline{H}_m = -\ell_m P_t^E/A_m = -\ (3.96)\ (26.8)/12.1 = -\ 8.87.$$

(3) Draw a line with slope $\overline{B}_m/\overline{H}_m = 8.87$ through the origin of the graph of the second quadrant of the Alnico 5 demagnetization curve (Figure 2).

(4) Find the magnet operating point at intersection (A) and value of $\overline{B}_m$ at that point, i.e., $\overline{B}_m = 5.14$ kG, as in Figure 2.

(5) Calculate total flux $\phi_t = \bar{B}_m A_m = 62.3$ k Mx.

(6) Find $\phi_G = P_G \phi_t / P_t^E = 23.3$ k Mx.

(7) Find $\bar{B}_g = \phi_B / A_G = 1.20$ kG.

So we see that the first and last two steps in this calculation must also be done for $SmCo_5$ and ϕ_t obtained from $\phi_t = F/R_t$ in lieu of step (5). But the time-consuming steps, (2) to (4), are unnecessary when REPM's are used, and no external aids such as graphs are then needed.

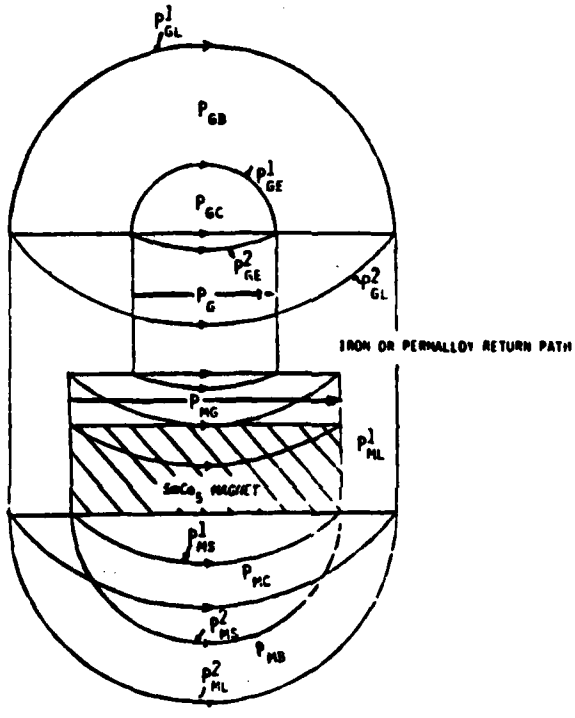

Figure 5a. Division of space around magnetic circuit into approximate flux paths.

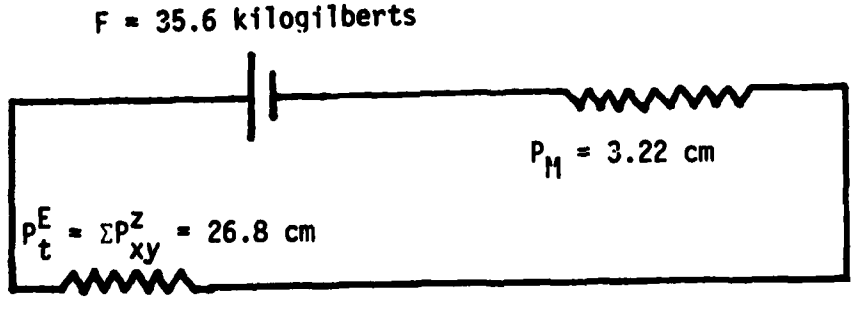

Figure 5b. Schematic of equivalent electric circuit.

TABLE 1. MAGNETIC FLUX PATHS OF FIGURE 5A.

PATH DESCRIPTION	PATHS	FORMULAE
GAPS WITH OPPOSING PARALLEL FACES	P_{MG}, P_G, P_M	$P = A_g/\ell_g$
PATHS BETWEEN PARALLEL, LINEAR EDGES OF OPPOSING SURFACES	P_{GE}^1, P_{GE}^2	$P = 0.26L$
ANNULAR, CYLINDRICAL SECTIONS EXTENDING BETWEEN COPLANAR SURFACE ACROSS A GAP	P_{GI}^1, P_{GI}^2, P_{MI}^1, P_{mI}^2	$P = \frac{L}{\pi} \ln(1+2t/\ell_g)$
SPHERICAL QUADRANTS ("ORANGE SLICES") CONNECTING OPPOSING CORNERS OF OPPOSING PARALLEL SURFACES	P_{GC}	$P = 0.77\ell_g$
QUADRANTS OF SPHERICAL SHELLS ("MELLON SLICES") CONNECTING COLINEAR EDGES SEPARATED BY A GAP	P_{GB} P_{MB}	$P = t/4$
SEMI-CYLINDRICAL SECTIONS BACKSTREAMING FROM THE SIDES OF THE MAGNETS	P_{MS}^1 P_{MS}^2	$P = 0.318y$
"ORANGE SLICE" SECTIONS BACKSTREAMING FROM LONGITUDINAL EDGES OF MAGNET	P_{MC}	$P = L/8$

IN THE FORMULAE: A_g and l_g refer to gap cross section areas and lengths, respectively; t to thicknesses of cylindrical and spherical shells, L to lengths of edges from which flux paths emanate, and y to the perimeter of the magnet.

Values of Permeances in Centimeters

$P_{MG} = 1.82$	$P_{GL}^1 = 3.18$	$P_{GC} = 0.292$	$P_{MS}^2 = 0.759$
$P_G = 10.16$	$P_{GL}^2 = 1.19$	$P_{GB} = 0.795$	$P_{MC} = 0.495$
$P_{GE}^1 = 2.64$	$P_{ML}^1 = 0.795$	$P_{MB} = 0.279$	$P_M = 3.22$
$P_{GE}^2 = 0.991$	$P_{ML}^2 = 0.199$	$P_{MS}^1 = 3.23$	$P_t^E = 26.8$

END

FILMED

1-83

DTIC